

## Quasar absorption lines

Pushpa Khare

*Physics Department, Utkal University, Bhubaneswar 751 004*

Received 12 April 1994; Accepted 9 August 1994

**Abstract.** Quasar absorption lines are an important tool to probe the universe at high redshifts, as they enable us to observe galaxies and intergalactic clouds at large distances, which are virtually inaccessible otherwise. This area of research is of great current interest and holds promise for the understanding of the large scale structure, and the evolutionary history of the universe. This article introduces the quasar absorption lines and describes their classification and properties. The interpretation of the properties in terms of models is briefly discussed. Some of the cosmological implications are stated.

*Key words:* quasars—absorption lines—redshift

### 1. Introduction

Absorption lines in the spectra of QSOs were first reported by Stockton & Lynds and Burbidge et al. in 1966. Since then, a large number of absorption lines have been observed in the spectra of several quasars. A typical quasar spectrum shows a power-law continuum with broad emission lines, with widths  $\sim 3000$ – $5000$  km s<sup>-1</sup>, occasionally reaching  $40,000$  km s<sup>-1</sup>, of ions like C IV, Si IV, Ly $\alpha$  etc. Superimposed on this are a number of narrow absorption lines with widths  $\sim 5$ – $100$  km s<sup>-1</sup>. A typical quasar spectrum is shown in Fig.1, taken from Wampler(1991). A careful analysis of these absorption lines, reveals that these lines actually fall into a number of groups, the lines belonging to an individual group presumably being produced by gas having a particular redshift, usually smaller than the emission redshift,  $z_{em}$ . Each group, termed as an absorption system with a particular absorption redshift,  $z_{ab}$ , typically consists of lines of Mg I, Mg II, C II, C IV, Fe II, Si II, Si IV, etc. Most of the lines longward of the Ly $\alpha$  emission line can be identified in this manner. It is to be noted that large number of absorption lines are observed because even though we are observing in the optical, we are actually seeing the *UV* part of the spectra in the rest frame of the absorber and a number of resonance lines of the abundant ions fall in the ultraviolet region. In

addition there are a large number of lines on the shorter wavelength side of the Ly $\alpha$  emission line. Most of these lines cannot usually be identified with any heavy element lines, and it is believed that these are lines in the Lyman series (mostly Lyman alpha) produced by neutral hydrogen clouds each with different redshift. The spectral region on the short wavelength side of the Lyman alpha emission line is crowded with these lines and is called the Lyman alpha forest.

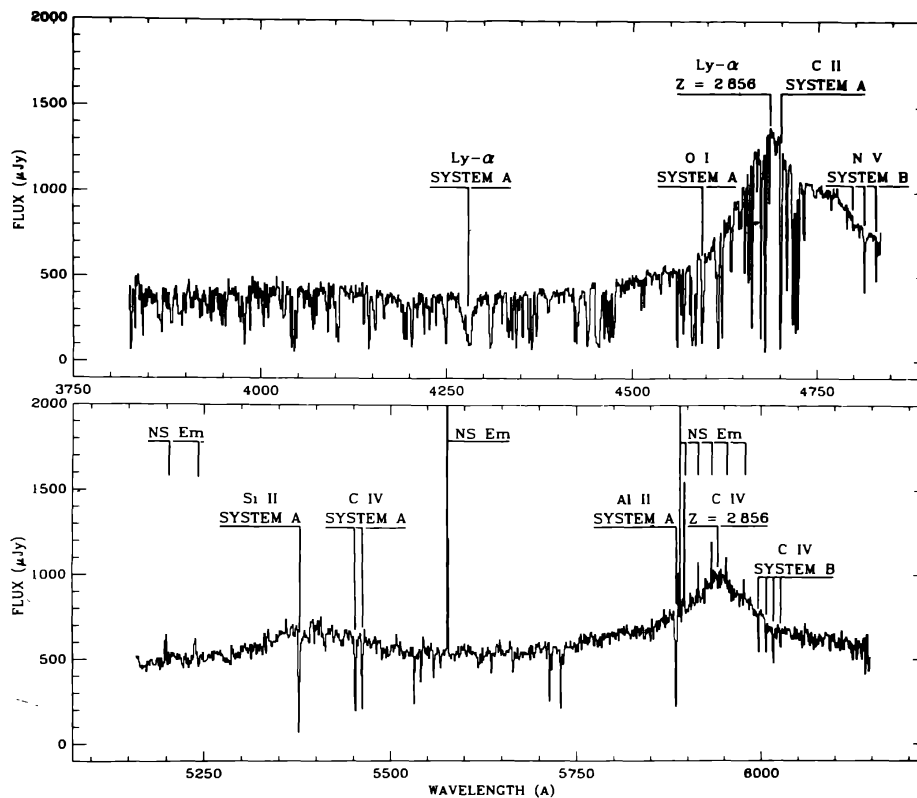


**Figure 1.** The spectrum of quasar UM 402 with emission redshift of 2.856. Lines denoted by NS Em are night sky emission lines. The spectrum shows Lyman alpha and C IV emission lines and several absorption lines belonging to absorption systems A and B with redshifts 2.523 and 2.88 respectively.

Even though absorption lines were first detected in 1966, a coherent picture was evolved in the late 80s due to two reasons.

- (i) The data was heterogeneous; different quasars were observed with different resolution over different wavelength ranges. Some selection effects were present and had to be identified and eliminated. Also there are different classes of absorption systems and it took long exposure times to collect large observational data set, and study their statistical properties.
- (ii) There was a long debate over the nature of the redshift of the absorption systems. There were two main hypotheses:

- (a) The intrinsic hypothesis: According to this hypothesis, the quasar absorption line systems (QSOALS) are produced by material intrinsic to the quasar, the difference in redshifts between the emitting and absorbing gas could occur due to the fact that the material producing the absorption lines is thrown out by the quasar with great velocities. This appeared quite likely in view of the energetic processes going on in the quasars.
- (b) The intervening hypothesis: The absorbing material is lying along the line-of-sight of the quasar; the absorption redshift being the cosmological redshift of the absorber. The material forming the heavy element lines could thus be sitting in the halos of the intervening galaxies as suggested by Bahcall & Spitzer (1969).

It is now widely accepted that most classes of absorption lines arise in intervening gas, the reasons being as follows:

- (1) Energetic constraints: Large differences between  $z_{ab}$  and  $z_{em}$  have been detected and require ejection velocities larger than  $0.5 c$  (Sargent et al. 1988a). The lower limit to the distance of the absorbing material from the quasar can be obtained in some cases from the absence of absorption lines from the fine structure levels of ions like C II, which gives an upper limit on the radiative excitation rates of these levels, thereby giving a lower limit on the distance of the absorbing material from the quasar. In some cases two quasars situated close to each other in the plane of the sky have absorption systems with identical absorption redshifts (Shaver & Robertson 1983). If the absorption is due to material ejected by the quasar, it must be in the form of a shell, the shell radius being larger than the transverse distance between the two quasars so as to cross both the lines-of-sight. The thickness of the absorbing shell can be estimated from the strength of the absorption lines. All these estimates can be combined to give the mass and therefore the kinetic energy of the shell, which in extreme cases, assuming spherical shells, is  $\sim 10^{62}$  ergs. It is difficult to envisage an ejection mechanism responsible for transfer of such a large amount of energy.
- (2) It was shown by a detailed study of absorption lines (Sargent et al. 1980; Young et al. 1982) that the absorbers are randomly distributed in redshift and the distribution of the absorbers bears no correlation with the properties of the parent quasar. Also the absorber distribution in the spectra of individual quasars is consistent with their belonging to the same parent population.
- (3) The most convincing support for the intervening hypothesis was provided by Bergeron (1988) by actually observing the galaxies close to the quasar line-of-sight, having redshift same as those of known absorption systems. In 80% of the chosen sample of absorption systems the absorbing galaxy was detected. The linear separation between the centre of the absorbing galaxy and the quasar line-of-sight was found to vary between 6 to 36 kpc (for  $H_0=100 \text{ km s}^{-1}$

Mpc<sup>-1</sup>). Since then other groups have also detected galaxies at the absorption redshift close to the quasar line-of-sight (Steidel 1993).

So, now it is widely accepted that most (except one class of systems as discussed below) of the absorption lines are produced by intervening galaxies and intergalactic clouds.

This then brings us to the importance of studying these lines. Galaxies being very faint can only be observed in their own light up to very low ( $z < 1.0$ ) redshifts. The important redshift range for the formation and evolution of galaxies is  $z > 2.0$ . The only way one can study the galaxies at such large redshifts seems to be through the absorption lines that they produce in the spectra of quasars. The interest in the study of these lines is rapidly growing and so are the observational data. This has resulted in a considerable progress in the understanding of the statistical properties of these lines and to some extent the nature of the absorbers producing these lines.

The study of these lines can provide the following information about the universe and in particular about galaxies at high redshifts.

- (1) Properties of galaxies: number density, sizes, clustering properties, temperature, density and ionization levels in the absorbing gas, chemical abundance and therefore star formation rates etc..
- (2) Intergalactic medium: properties of primordial clouds, their distribution, abundance etc..
- (3) Metagalactic *UV* radiation field.
- (4) Evolution in all the above.
- (5) Large scale structure of the Universe.
- (6) Magnetic fields in galaxies at high redshifts.
- (7) Quasar activities.

## 2. Method of study

Before going into the details of the classification and the properties of QSOALS we will briefly discuss the curve-of-growth analysis which is essential for the understanding of the properties of QSOALS.

Absorption lines are produced whenever, cool gas is present along the line-of-sight to a hot light source. The atoms/molecules and ions in the cool gas, absorb photons of characteristic frequency from the continuum radiation falling on them and the radiation coming out of such a gas has dark lines superimposed on the continuous spectrum of

the source. The strength of an absorption line is measured by its equivalent width, which is a measure of the area covered by the line profile and is defined as the width that a line would have if its profile was rectangular and at every point inside, light was completely absorbed as shown in Fig. 2. Line strength and therefore equivalent width depends upon the amount of cold matter present in the path of light, measured by the column density,  $N \text{ cm}^{-2}$ , which is the number of absorbing atoms/ions in a cylinder with unit cross-section extending from observer to the source. Larger the column density of a particular species, higher will be the equivalent width of absorption lines produced by that species. In addition to the column density the line strength also depends upon the absorption cross-section and the thermal and dynamical state of the absorbing gas. The relation between equivalent width and the number of absorbing atoms/ions i.e. the column density is called the curve-of-growth. Such a relation is required to determine the column density in the absorbing gas from the equivalent width measured from observations.

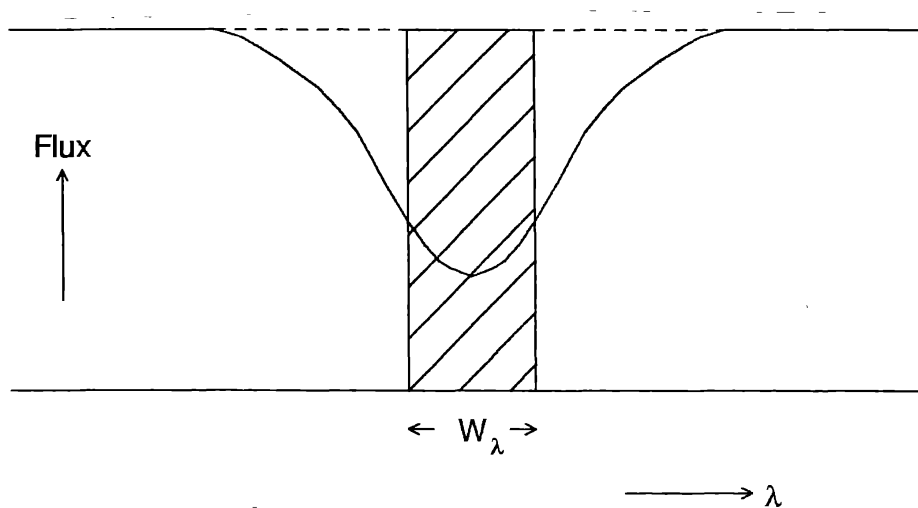


**Figure 2.** A schematic plot of energy distribution in the neighbourhood of an absorption line. The equivalent width  $W_\lambda$  is the width of the rectangular line with the same total absorption as the actual line.

The equivalent width can be written in terms of the intensity of flux of light  $I_\nu^c$  incident on the absorbing gas and the emergent intensity  $I_\nu$  at frequency  $\nu$ , as

$$W_\nu = \int \frac{(I_\nu^c - I_\nu)}{I_\nu^c} d\nu \quad (1)$$

the integral being over the width of the line.

The intensity is defined as the amount of energy crossing unit area, per unit time, per unit frequency interval, per unit solid angle. Assuming no reemission from the absorbing gas, the decrease in the incident intensity after travelling a distance  $dl$ , in the absorbing gas, is proportional to (i) the incident intensity, as more the number of photons more is the probability of absorption (ii) the absorbing properties of the gas,

quantified by the absorption coefficient  $k_\nu$  ( $\text{cm}^{-1}$ ) (iii) the thickness  $dl$  of the absorbing layer. We can thus write.

$$dl_\nu = -K_\nu I_\nu dl. \quad (2)$$

It is convenient to define a dimensionless quantity, the optical depth  $\tau_\nu$ , as

$$d\tau_\nu = k_\nu dl. \quad (3)$$

Integrating equation(2)we get the emergent intensity as

$$I_\nu = I_\nu^c e^{-\tau_\nu}. \quad (4)$$

Here,

$$\tau_\nu = \int_0^L d\tau_\nu = k_\nu L, \quad (5)$$

for uniform absorbing medium of length  $L$  and is a measure of the extinction of the incident intensity by the absorbing column. The equivalent width is given in terms of the optical depth by

$$W_\nu = \int (1 - e^{-\tau_\nu}) d\nu. \quad (6)$$

The absorption coefficient can be written as

$$k_\nu = n\sigma_\nu, \quad (7)$$

where  $n$  is the number of absorbing particles per unit volume, all assumed to be at rest with respect to the observer and  $\sigma_\nu$  is the absorption cross-section at frequency  $\nu$ , which is given by,

$$\sigma_\nu = \frac{\pi e^2}{m_e c} f \phi_\nu. \quad (8)$$

Here  $f$  is the oscillator strength,  $m_e$  is the electron mass and  $\phi_\nu$  is the normalized line profile function given by

$$\phi_\nu = \frac{\gamma/4\pi^2}{(\nu - \nu_0)^2 + \left(\frac{\gamma}{4\pi}\right)^2}. \quad (9)$$

This shape of the line is due to the fact that the excited states of an atom/ion have a finite width due to natural broadening,  $\nu_0$  is the line centre frequency and  $\gamma$  is the damping constant. If the absorbing particles are not at rest but are moving with thermal velocities at a temperature  $T$ , then the line profile gets modified, as each absorbing particle has the above line profile in its own rest frame, and is given by,

$$\phi\nu = \frac{\gamma}{4\pi^{2.5} b} \int_0^{\infty} \frac{\exp(-\nu^2/b^2)}{\left(\nu - \nu_0 - \frac{\nu}{c} \nu\right)^2 + \left(\frac{\gamma}{4\pi}\right)^2} d\nu. \quad (10)$$

Here the velocity dispersion parameter  $b$  is given by

$$b = b_{th} = \sqrt{\frac{2KT}{m}}. \quad (11)$$

where  $m$  is the mass of the absorbing particle.

If in addition to thermal motion, the absorbing gas has turbulent motion and if the turbulent velocities have a gaussian distribution then the resulting velocity distribution can be obtained by folding the turbulent velocity distribution with the thermal velocity distribution, which will also be a Gaussian, with velocity dispersion given by

$$b^2 = b_{th}^2 + b_{turb}^2. \quad (12)$$

The profile given in equation (10) is known as the Voigt profile. Equations (6–8) and (10) give a relation between  $W$  and  $N$  or the curve-of-growth. Obviously the relation depends on the value of  $b$ . The curve of growth for Mg II  $\lambda$  2796 Å is given in Fig.3. Analytic relations between  $W$  and  $N$  can be obtained in three different ranges of column density as follows:

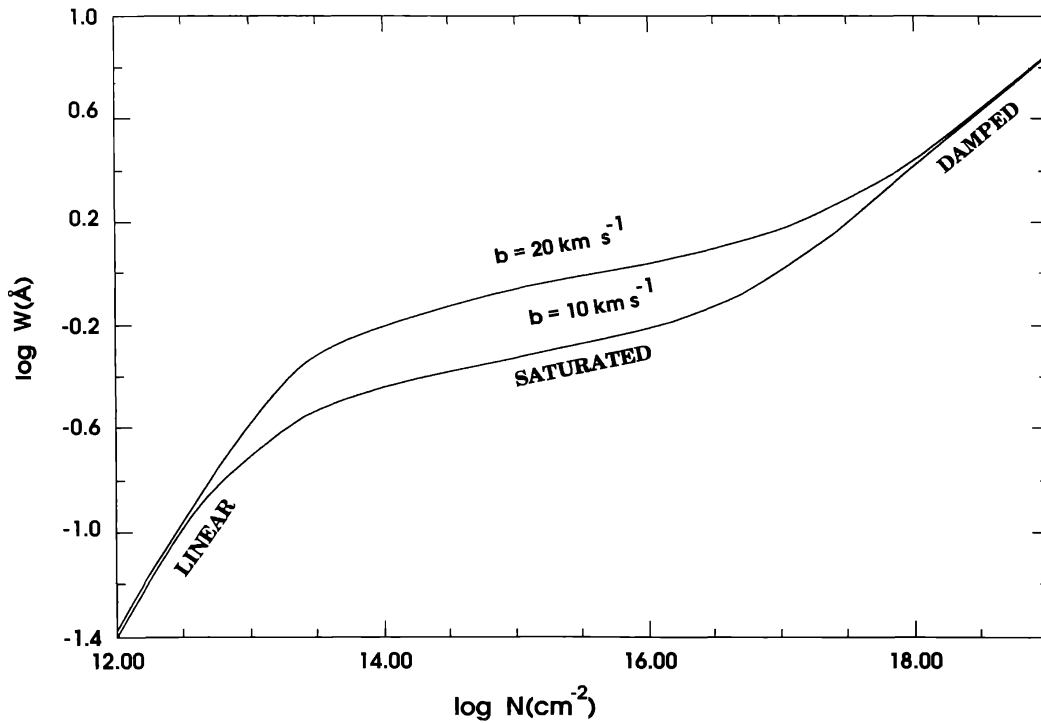


**Figure 3.** Curve-of-growth for Mg II  $\lambda$  2796 Å for two values of velocity dispersion parameter. The linear, saturated and damped portions are indicated.



(1) Optically thin case : The absorbing gas has an optical depth,  $\tau_\nu \ll 1$ . The line is weak and equivalent width is given by

$$W_\lambda = W_\nu \frac{c}{v_0^2} = \lambda_0^2 \frac{\pi e^2}{m_e c^2} N f . \quad (13)$$

This is known as the linear portion of the curve-of-growth as  $W_\lambda$  is directly proportional to the column density.

(2) Optical depth  $\sim 1$  : This is the region where the absorbing gas is just beginning to become optically thick. Here

$$W_\lambda = \frac{2\lambda_0 b}{c} \left[ \ln \left( \frac{N \sqrt{\pi} e^2}{m_c} / \frac{f \lambda_0}{b} \right) \right]^{1/2} \quad (14)$$

In this region the increase in  $W_\lambda$  with  $N$  is very slow and this part of the curve of growth is known as flat portion or logarithmic portion or saturated portion of curve-of-growth. The lines with equivalent widths in this range are said to be saturated and the equivalent widths depend on  $b$ , being higher for higher  $b$  for a given  $N$ .

(3) Optically thick case : The optical depth is very large  $\tau_\nu \gg 1$ . In this part the wings of the line due to natural broadening become very prominent. Here

$$W_\lambda = \frac{2\lambda_0^2}{c} \left( \frac{4\pi^2 e^2}{m_c} N f \gamma \right)^{1/2} , \quad (15)$$

and the rate of increase of  $W_\lambda$  with  $N$  though slower than the linear portion is faster than the saturation portion. This part is called damped or square root portion of the curve-of-growth and the lines falling on this part of the curve-of-growth are called damped lines.

The observation of equivalent width of a single line can give us the column density of the absorbing gas only if the lines lies on the linear or the damped portion of the curve-of-growth as the saturation portion depends on the unknown parameter  $b$ . The C IV and Mg II lines being doublets have an advantage as two lines from the same lower level (ground state) of the same ion are observed. The wavelengths of these lines are also very similar and the difference in their equivalent widths is due to the different oscillator strengths of these two transitions. The doublet ratio (DR) i.e. the ratio of equivalent widths of the two lines of the doublet, is a constant if the two lines lie on the linear or on the damped portion of the curve-of-growth. If the lines are saturated then the ratio depends on the velocity dispersion parameter and the knowledge of DR along with the equivalent widths can enable a determination of  $b$  and therefore the column density of the absorbing atoms/ions. This is called the doublet ratio analysis. Essentially similar technique is used in the so called curve-of-growth analysis in which  $\log (W_\lambda / \lambda)$  is plotted against  $\log N \lambda f$ . Such a curve will be identical for



all species in the linear and saturated portion. The observations of lines of different species can therefore be combined together and analysed using this curve-of-growth to obtain the column densities and the  $b$  value (assuming the  $b$  value is same for all the species). High resolution observations give the information about the line profile and it is possible to obtain the column densities of the absorbing particles and their  $b$  values by fitting the observed profiles with a Voigt profile.

### 3. Classification of QSOALS

QSOALS can be classified in the following five classes. The last three classes are often grouped together and are called the metal line systems.

- (a) Associated systems. (b) Lyman alpha forest lines. (c) Heavy element lines.
- (d) Lyman limit systems. (e) Damped Lyman alpha systems.

#### (1) Associated systems

This is the class, referred to earlier, which is believed to be formed by material intrinsic to the quasar. These include two types of lines :

- (1) Broad absorption lines (BAL) : These are very broad lines with widths of several thousands of  $\text{km s}^{-1}$  starting on the immediate blueward side of the corresponding emission lines as shown in Fig.4, taken from Turnshek (1988). These are typically from highly ionized atoms like N V, C IV etc. 15% of the BAL QSOs also show lines from atoms in low stages of ionization, like Mg II, Al II, Fe II etc. The close association of these lines with the emission lines and the fact that these lines never occur at redshifts very different than the emission redshifts, indicates that they are produced by material intrinsic to the quasars. These absorption lines only occur in radio quiet quasars. It is not yet clear if the BAL QSOs are a subclass of quasars or they produce BAL due to orientation effects. Roughly 10% of all quasars show these phenomenon and it is possible that the clouds producing these absorption lines are present around all quasars but with a covering factor of  $\sim 0.1$ . An upper limit  $\sim 0.2$  on the covering factor can be obtained from the absence of any detectable emission from the gas producing this absorption. Assuming that the number of photons absorbed is equal to the number of photons emitted, this lack of emission gives an upper limit on the total number of photons absorbed and therefore on the amount of absorbing gas and the filling factor. The abundance of metals in BAL QSOs is found to be enhanced compared to the solar abundance by factors up to 100. Some correlation has been found between the emission line properties of quasars and the occurrence of BAL, like C IV is weaker and N V, Al III, Fe II is stronger in BAL QSOs.
- (2) Strong narrow lines with  $z_{\text{ab}} \sim z_{\text{em}}$ : There are more lines with  $z_{\text{ab}} \sim z_{\text{em}}$ , than expected on the basis of intervening hypothesis. These are systems with

relative velocities between the emitting and absorbing gas  $< 5000 \text{ km s}^{-1}$ . These could be formed by material thrown out by the quasar or by the host galaxy or other galaxies in the cluster containing the quasar. There is some indication that these systems occur preferentially in radio loud quasars. Some evidence for these systems to be strong in C IV has also been obtained (Barthel 1991). The study of associated systems can give us an idea about the activities going on in the quasar.

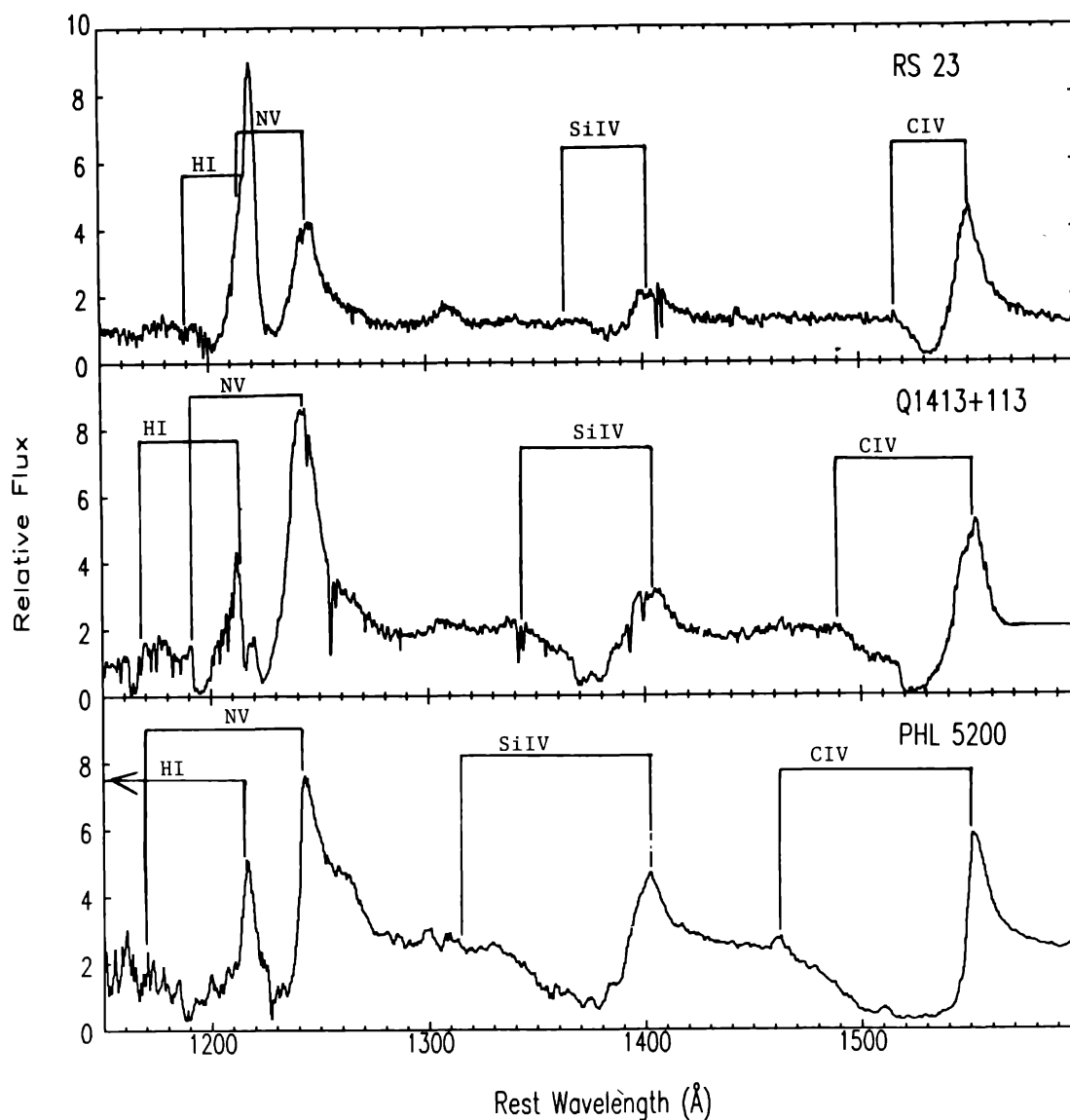


**Figure 4.** Spectra of three quasars showing broad absorption lines of C IV, Si IV, N V and H I.

We will not discuss these systems further and will concentrate on the 'intervening systems' in the rest of the article.

## (2) Lyman alpha forest lines

These are the most numerous QSOALS and form > 90% of all the absorption lines observed. A typical Lyman alpha forest can be seen in Fig.1. These lines are simply too numerous to be formed by galactic halos (one will need too many of them or they have to be too large with radius ~0.4 Mpc) and so are believed to be formed by intergalactic clouds. Another reason for believing this is the fact that no heavy element lines at the redshift of these lines have been observed indicating that they are primordial clouds which have not undergone nucleosynthesis. Being so numerous, it is easy to collect large samples of these lines (one has to observe only a few quasars, as there may be hundreds of these lines in a single quasar) and study their statistical properties. As we will see below, this has led to important information about the nature of IGM, and intensity of the metagalactic *UV* background radiation.

## (3) Heavy element systems

These form only 5% of the QSOALS but are important as these are believed to have been formed in material belonging to the intervening galaxies. These are easily identified due to the presence of C IV or Mg II doublets and most of the lines on the long wavelength side of Lyman alpha emission line are usually identified. It is to be noted that C IV (1550 Å) and Mg II (2796 Å) are present in very different regions of spectra and can be observed in optical over different redshift ranges. Mg II can be observed for redshifts  $0.2 < z < 2.1$  while C IV can be observed  $1.2 < z < 4.0$ . The redshift ranges are not exclusive and both can be simultaneously observed over a narrow redshift range  $1.2 < z < 2.1$ . Large samples of Mg II systems and C IV systems have been collected by several observers (Sargent et al.1988a, 1988b).

## (4) Lyman limit systems (LLS)

Some quasar spectra, when observed sufficiently to the shorter wavelength side of Ly $\alpha$  emission, exhibit a sudden discontinuity in the spectra, the intensity suddenly becoming close to zero at shorter wavelengths. This is believed to be produced by absorbing gas with high column density of neutral hydrogen  $> 2 \times 10^{17} \text{ cm}^{-2}$ , having  $\tau_{912\text{\AA}} > 1.0$ . Such gas will absorb all photons shortward of 912Å in its rest frame, producing discontinuity in the observed spectra at  $\lambda_{\text{LLS}} = 912(1 + z_{\text{LLS}})\text{\AA}$ . So if one observes a discontinuity in the spectra of a quasar at  $\lambda_{\text{LLS}}$ , one can get the absorption redshift of the cloud producing it and then look for the presence of heavy element lines at that redshift. These lines are often found and form what is called Lyman limit system. It is found that most of the LLS do have accompanying heavy element lines, the remaining few may be produced by the high column density tail of the Lyman alpha forest clouds. Fig.5 taken from Sargent et al. (1989), shows the Lyman limit

discontinuity for Q 0001 + 087. The LLS form an important class of the quasar absorption lines due to the following reasons.

- (i) Their presence is exhibited by a sudden discontinuity in the spectra and therefore they can be detected even in low resolution spectra. IUE observations can thus reveal the presence of these systems and with these one can detect LLS with  $0.4 < z_{\text{LLS}} < 2.2$ . With ground based telescopes one can observe  $2.5 < z_{\text{LLS}} < 4.7$ . Thus LLS can be observed over the entire range of redshift from 0.4–4.7 and are very useful to study the evolution of absorbers.

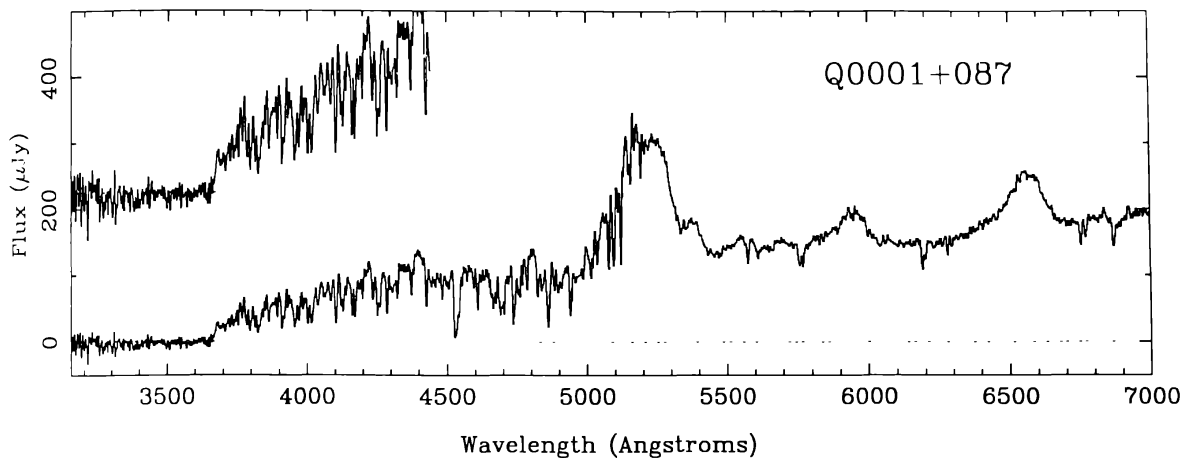


**Figure 5.** Lyman limit discontinuity for  $Z_{\text{LLS}} = 3.007$  in the spectra of quasar Q 0001 + 087. The plot in the upper left hand corner shows a magnified view of the discontinuity.

- (ii) The column density being large, lines of both high and low ionization as well as Lyman series can be observed and it is possible to model the ionization equilibrium of the system to obtain the physical conditions and nature of the clouds producing these systems.

#### (5) Damped Lyman alpha systems

A damped Lyman alpha line for Q 0201 + 365 is shown in Fig.6 taken from Savaglio et al. (1993). These systems are characterized by Ly $\alpha$  lines with  $N_{\text{HI}} > 2 \times 10^{20} \text{ cm}^{-2}$  so that the lines lie on the damped portion of the curve-of-growth and can be identified due to the presence of damping wings. The wings cannot be produced by the blending of weaker lines. These are always accompanied by heavy element lines.

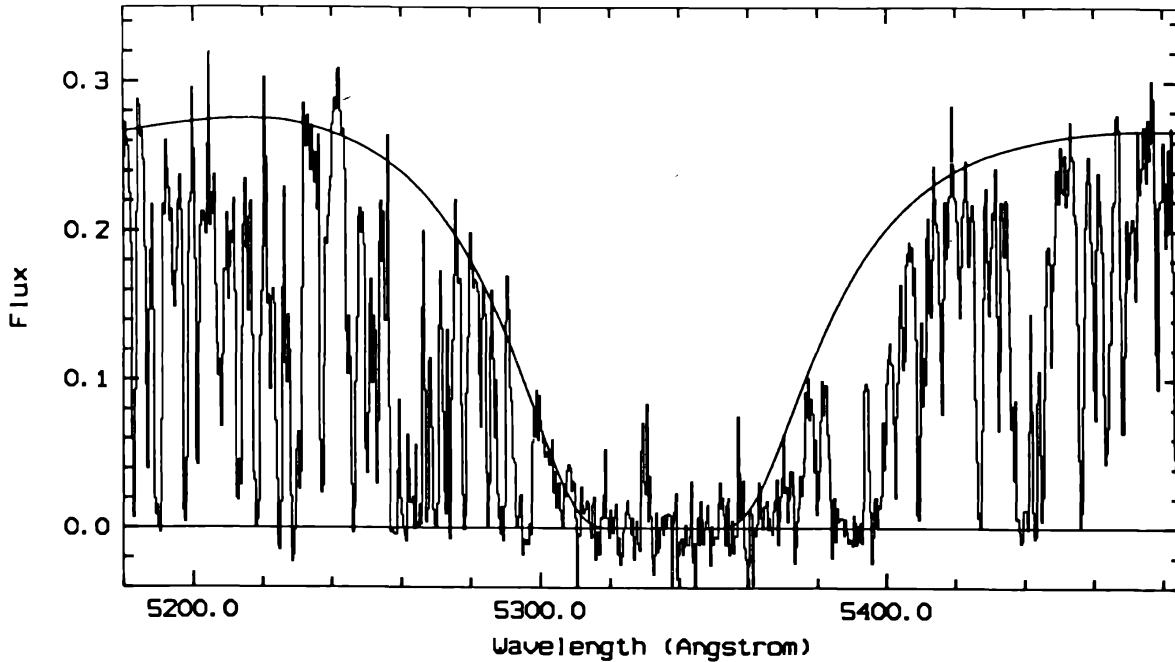


**Figure 6.** Damped Lyman alpha line  $z_{ab} = 3.39$  in the spectra of Q 0000-2619. The best fit Voigt profile is also shown.

#### 4. Properties of QSOALS

Homogeneous samples of QSOALS belonging to a given class, observed with similar resolution and S/N ratio, free of selection effects and obtained using similar criterion for line identification, often limited by a rest equivalent width cutoff, are studied for the following properties.

##### (1) Redshift distribution

The number of absorption lines (systems) per unit redshift interval per line-of-sight, usually designated as  $dN/dz$  can be obtained for observed homogeneous samples. Its redshift dependence is usually written as

$$\frac{dN}{dz} = \frac{dN}{dz} \Big|_{z=0} (1+z)^\gamma. \quad (16)$$

Theoretically, for randomly distributed intervening absorbers one can write (Peterson 1978)

$$\frac{dN}{dz} = cH_0^{-1} \phi(z) \sigma(z) (1+z) (1+2q_0z)^{-1/2}. \quad (17)$$

Here  $\phi(z)$  and  $\sigma(z)$  are the comoving number density and absorption cross-section of the absorbers,  $c$ ,  $q_0$  and  $H_0$  are the velocity of light, deceleration parameter and Hubble constant respectively. For  $q_0 = 0.5$ , equation (17) gives,

$$\frac{dN}{dz} = cH_0^{-1} \phi(z) \sigma(z) (1+z)^{1/2}. \quad (18)$$

Thus the observed value of  $\gamma$  can yield information about the change of absorber properties, namely  $\phi(z)$  and  $\sigma(z)$  with redshift. The observed value of  $dN/dz$  at a given redshift can yield values of  $n(z)$   $\sigma(z)$  at that redshift.

### (2) Equivalent width and column density distribution

The number of absorption lines of a particular species per unit rest equivalent width interval around an equivalent width  $W$ ,  $f(W)$ , can be obtained as a function of  $W$  from observations. This observed equivalent width distribution is usually parameterized in two ways

$$f(W) dW = \frac{N^*}{W^*} e^{-\frac{W}{W^*}} dW, \quad (19)$$

and

$$f(W) dW = KW^{-\delta} dW, \quad (20)$$

$N^*$ ,  $W^*$ ,  $K$  and  $\delta$  being constants. The equivalent width can be converted to column density distribution by using the doublet ratios or by profile fitting method and it is possible to obtain the column density distribution,  $f(N)$ , for a particular species which is usually parameterized as

$$f(N) dN = KN^{-\beta} dN. \quad (20)$$

### (3) Clustering properties

It is observed that the absorption line systems tend to occur in clumps, with lines occurring close to each other in redshift along a line-of-sight. This can be quantified by defining a two point correlation function over a redshift interval  $\Delta z$  as the excess probability of finding an absorption system in a redshift interval  $\Delta z$  around  $z$ , over that for uniformly distributed absorbers.

## 5. Properties of Lyman alpha lines

These lines are found to evolve strongly with redshift, the evolutionary parameter,  $\gamma$  being  $\sim 2.36-2.75$ . Close to individual quasar, however, a departure from this is observed, the number of lines per unit redshift range, decreasing with redshift. This so

called inverse effect or proximity effect is attributed to the fact that Lyman alpha clouds close to the quasars are highly ionized due to the increased *UV* radiation (from the quasar) above the general intergalactic *UV* background and do not have sufficient neutral hydrogen to produce observable Lyman alpha lines. From a knowledge of the quasar *UV* radiation field, the proximity effect can be used to obtain the intensity of the background *UV* radiation at the quasar redshift. Such a study indicates that the background field is  $\sim 10^{-21}$  erg s<sup>-1</sup> cm<sup>-2</sup> sr<sup>-1</sup> Hz<sup>-1</sup> and is roughly constant in the redshift range 1.7–3.8 (Bajtlik et al. 1988; Lu et al. 1991). At lower redshifts  $\sim 0.5$  the proximity effect shows that the background field is much lower  $\sim 6 \times 10^{-24}$  erg s<sup>-1</sup> cm<sup>-2</sup> sr<sup>-1</sup> Hz<sup>-1</sup> (Kulkarni & Fall 1993). The observed quasars cannot produce the strong background radiation at high redshifts and an additional source of *UV* radiation, either young star-forming galaxies or quasars obscured from us by intervening dust have been proposed. Some evidence of differential evolution, with  $\gamma$  depending on the equivalent width has been obtained (Trevese et al. 1992; Acharya & Khare 1993)

The equivalent width distribution of Lyman alpha lines follows the exponential law and the power law index of neutral hydrogen column density distribution is  $\sim 1.5$ . Lyman alpha clouds are not found to be clustered, however a weak clustering has been reported on scales of 300 km s<sup>-1</sup> (Webb 1987). This lack of clustering is consistent with their not being formed in galaxies as the galaxies are known to be clustered. The sizes of Lyman alpha clouds have been obtained to be  $\sim 5$ –25 kpc (Foltz et al. 1984; Smette et al. 1992) from the observations of common Lyman alpha lines in the spectra of double images of gravitationally lensed quasars. Typical neutral hydrogen column densities in these clouds are  $< 10^{16}$  cm<sup>-2</sup> thus the density of neutral hydrogen is  $< 10^{-7}$  cm<sup>-3</sup>. If the clouds are in photoionization equilibrium with ionizing radiation field, as given by the proximity effect, then electron densities  $\sim 10^{-3}$  cm<sup>-3</sup> and temperature  $\sim 10^4$  K are indicated giving cloud masses  $\sim 10^7$ – $10^8$  M<sub>⊙</sub>. The main three types of models for these clouds, considered in the literature are as follows.

- (1) The Lyman alpha absorbers are in pressure equilibrium with hot and tenuous intergalactic medium (Sargent et al. 1980). The clouds are photoionized by the intergalactic background *UV* radiation and expansion of the clouds due to cosmic expansion may explain the observed redshift distribution. Ikeuchi and Ostriker (1986) have proposed that such clouds may be formed by fragmentation of dense shells produced by explosions, occurring on large scale at the sites of QSOs or newly formed galaxies.
- (2) A freely expanding model for the Lyman alpha clouds has been proposed by Bond et al. (1988). In this model, the clouds, instead of being in pressure equilibrium with the intergalactic medium are expanding freely. The rate of expansion is however too large and it is difficult to reproduce the redshift distribution as well as column density distribution.
- (3) The clouds may be gravitationally confined by dark matter (Rees 1986). Clouds of masses  $\sim 10^8$  M<sub>⊙</sub> are formed in large numbers in cold dark matter dominated universe. The column density distribution is well explained in this model. The



redshift distribution can be attributed to the evolution in the background *UV* flux as well as the merging of these clouds.

The understanding of the nature of these clouds will provide important information about galaxy formation.

## 6. Properties of heavy element systems and LLS

Large homogeneous samples of these lines have been compiled by Sargent et al. (1988a, 1988b), Steidel & Sargent (1992), Lanzetta et al. (1987) etc. These have been analysed to obtain properties of these absorbers described below.

Assuming that these systems are produced by galaxies, equation (17) can be used to give an estimate of their effective radii  $R$  for producing absorption lines of various kinds, from the observed values of  $dN/dz$  and the present value of galaxy number density (and assuming that this has remained unchanged over the relevant redshift range). At  $z \sim 2.0$  and assuming  $H_0 = 100 \text{ km s}^{-1} \text{ Mpc}^{-1}$ , this gives  $R_{\text{C IV}} \sim 90 \text{ kpc}$ ,  $R_{\text{Mg II}} \sim 50 \text{ kpc}$  and  $R_{\text{LLS}} \sim 75 \text{ kpc}$ . These large halo sizes are consistent with the direct observations of absorbing galaxies by Bergeron (1988) and Steidel (1993). LLS are produced by absorbers with column density of neutral hydrogen  $> 10^{17} \text{ cm}^{-2}$ . Assuming that the gas is photoionized by *UV* radiation, a similar amount of neutral hydrogen is also needed to produce Mg II column densities indicated by the Mg II absorption lines. The number of these systems per unit redshift interval and its evolution with redshift (as discussed below) is also found to be similar. It is therefore believed that LLS and Mg II systems originate in a single class of absorbers. The equivalent width distribution of Mg II and C IV lines is consistent with the exponential distribution. The distribution is found to be changing with redshift indicating that the fraction of stronger Mg II systems was higher in the past, opposite being the case for C IV (Caulet 1989; Steidel 1990).

High resolution observations of the absorption lines have revealed that the lines are actually made up of several components which typically span a relative velocity range of  $< 200 \text{ km s}^{-1}$  as shown in Fig.7, taken from Blades (1988). This is interpreted as being due to the presence of clouds in the galactic halos, each line component being produced by an individual cloud. The doublet ratios for C IV and Mg II, are found to be uncorrelated with the equivalent widths of these systems, confirming the cloudy nature of the halo, the higher equivalent width lines (observed with low resolutions) being formed by a larger number of clouds rather than a single cloud with higher column density. Observed equivalent width is thus a likely measure of the number of clouds. Note that if the higher equivalent widths were due to larger column densities in the clouds, the doublet ratio, which decreases with increasing column density would have shown an anti-correlation with equivalent width.

The C IV and Mg II absorption lines show significant clustering on velocity scales  $< 600 \text{ km s}^{-1}$ . The clustering scale is similar to that of galaxy-galaxy correlation and is also taken to be an evidence in favour of galactic origin of these lines.

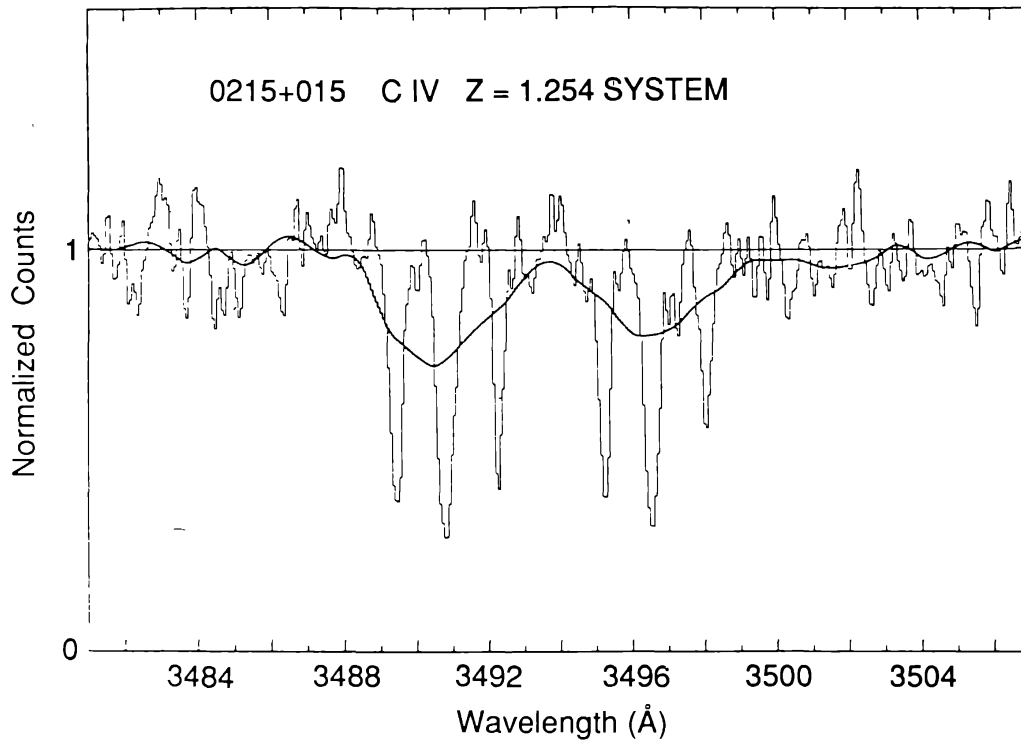


**Figure 7.** A comparison of the C IV doublet in Q 0215+015 obtained at low (dark curve) and high (light curve) resolution. The multicomponent nature is evident at high resolution.

Attempts have been made to infer the ionization states of absorbers by searching for Mg II absorption lines at the redshift of C IV systems and vice versa. Steidel & Sargent (1992) based on data for  $\sim 100$  such systems conclude that in 26% of the systems, lines from both singly ionized (Mg II) as well as highly ionized (C IV) species are present while in 73% of the systems, lines of only highly ionized species are present. Only 1% of the systems show lines of singly ionized species not accompanied by lines of C IV, Si IV etc.

Assuming single clouds to be responsible for producing the observed Lyman limit systems at  $z \sim 3.0$ , Steidel (1990) compared the observations of column densities of various ions with results of detailed photoionization models and found the cloud parameters to be  $0.01 < n_H < 0.1 \text{ cm}^{-3}$ ,  $1 < D_c < 15 \text{ kpc}$ ,  $10^6 < M_c < 10^9 M_\odot$  and  $-3.0 < [M/H] < -1.5$ ,  $D_c$  and  $M_c$  being the cloud diameter and mass respectively and  $(M/H)$  is the metallicity in the clouds. Srianand & Khare (1993, 1994) have constructed models for galactic halos filled with clouds, the cloud density and heavy element abundance in clouds decreasing with increasing distance of the clouds from the galactic centre. They found that assuming a range in cloud sizes and ionization parameters it is possible to produce the observed properties of C IV as well as Mg II systems, neutral hydrogen column density distribution over the range covered by LLS to the damped

Lyman alpha systems, as well as the ratios of equivalent widths of several lines observed in such systems. The radii of individual clouds are  $\sim 0.3\text{--}3.0$  kpc with column densities of hydrogen  $\sim 10^{20}\text{--}10^{21}$   $\text{cm}^{-2}$ . Number of clouds is  $\sim 700\text{--}70,000$ . The total mass of the halo is found to be  $\sim 10^{10}\text{--}10^{11}M_{\odot}$ . Steidel & Sargent (1992) have pointed out that the collision time scales of clouds in the halo, having random velocities  $\sim 200$   $\text{km s}^{-1}$ , as shown by the relative velocities between components of lines in an absorption system, will be typically  $\sim 5 \times 10^8$  yr and may be smaller than the dynamic time scale leading to dissipation and infall of the cloud material towards the galactic centre. They suggest that the rate of infall may however be small due to cloud compression, and cooling during collisions, resulting in star formation. The energy released during star formation may be able to sustain the clouds in the halo for time periods covering the redshift range 4 to 0 over which the absorption lines have been observed. York et al. (1986) have argued that the galaxies are surrounded by dwarf galaxies with star forming regions which are responsible for producing the complex velocity structures in the absorption lines. Such regions have been observed as concentration of emission line (O II) regions near QSO absorbers (Yanny & York 1992).

The observed redshift distribution and the evolutionary parameter  $\gamma$  obtained from these, for LLS, Mg II and C IV systems are shown in Fig.8, taken from Steidel (1992). The values of  $\gamma$  are similar for the LLS and the Mg II absorbers and are consistent with non-evolving absorbers. The C IV systems on the other hand show a different behaviour. Negative value of  $\gamma$  shows that  $\phi(z) \sigma(z)$  decreases with redshift. Steidel et al. (1988) have interpreted this as being due to lower abundance of carbon in the past and have concluded that the observed value of  $\gamma$  indicates an increase in the chemical abundance of carbon by a factor of  $\sim 2$  from  $t = 1.5$  Gyr to 4 Gyr. More detailed calculations taking into account the effect of changing of radiation field with redshift by Khare & Rana (1993) show that the abundance evolution may be much more rapid, the abundance increasing by a factor of 5–20 in the time period mentioned above.

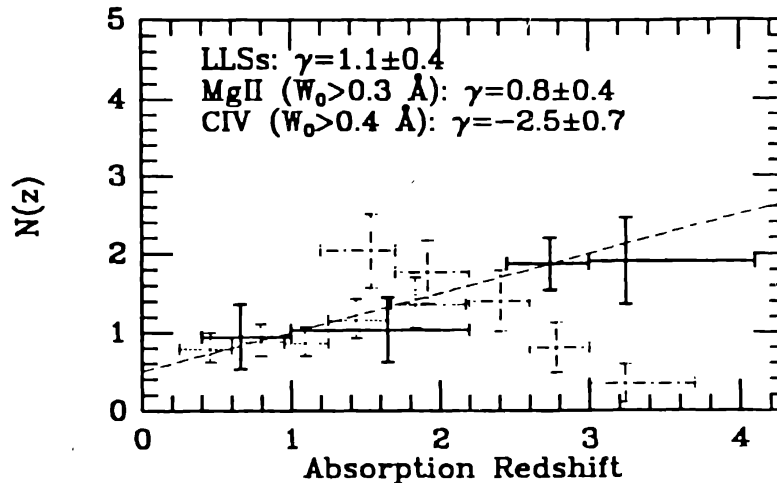


**Figure 8.** The redshift distribution of LLS, Mg II and C IV systems shown by solid, dotted and dashed lines respectively. The inferred values of  $\gamma$  are also shown.

## 7. Properties of damped Lyman alpha systems

Large samples of damped Lyman alpha systems have been compiled by Lanzetta et al. (1991). Assuming these systems are produced by galaxies the observed  $dN/dz$  shows the effective radius of the galaxy for production of damped Lyman alpha lines to be  $\sim 22$  kpc. The column density distribution of neutral hydrogen ( $\beta = 1.67 \pm 0.19$ ) is very similar to that of Lyman alpha forest clouds as well as that of metal systems, the average column densities being  $\sim 10^{21} \text{ cm}^{-2}$ . Several of these have been observed in absorption at radio wavelengths  $= 21(1 + z)$  cms. Evidence of dust with an amount about a tenth of that in the interstellar medium and magnetic fields of a few microgauss in these systems have been obtained. The particle density in the absorbers producing these systems, estimated from the ratio of column density of C II\* to that of C II is found to be  $\sim 1 - 10 \text{ cm}^{-3}$ . The metal abundances of several damped Lyman Alpha systems have been determined by Pettini et al. (1994) by observing zinc lines in these systems at  $z \sim 2$ . The typical metallicity is found to be approximately 1/10 solar. There is a considerable range spanning one to two orders of magnitude in metallicity at a given epoch. The mass density contributed by these systems is higher than that contributed by all other types of lines put together and is similar to the mass density of luminous matter in the spiral galaxies. It is therefore believed that these are the progenitors of spiral galaxies. If correct this has important implications about galaxy formation theories as it indicates that disks formed early, were large initially and later contracted to the present day sizes.

## 8. Cosmological implications

### (a) Properties of high redshift galaxies

Bergeron & Boisse (1991), Bergeron et al. (1992) and Steidel (1993) have directly observed galaxies producing Mg II absorption lines at redshifts 0.4 – 1.0 by deep imaging and follow up spectroscopy. For a sample of 40 galaxies with  $\langle z \rangle = 0.6$ , Steidel (1993) has shown that the optical and optical/infrared colours of these galaxies are consistent with mid to late type spiral galaxies. Very red or very blue galaxies are generally absent. Brighter galaxies tend to have larger impact parameters. The distribution of impact parameters is consistent with spherical halos with a luminosity dependent radius given by  $R(L) = 35 h^{-1} (L/L^*)^{0.2}$  kpc. The absorption line properties are well correlated with impact parameter. He concludes that absorption line selection is probably the most powerful criterion for isolating examples of very high redshift galaxies.

### (b) Large scale structure of the universe

Four nearby quasars Tol 1035–2737, Tol 1037–2704, Tol 1038–2707 and Tol 1038–2712, lying close to each other in the plane of the sky and also having redshifts close to 2.2 are found to have several  $\sim 5$  absorption lines within a narrow absorption redshift range from 1.89 – 2.14. The probability of this happening by chance in a uniform distribution of absorbers is very small. It thus appears that there is a supercluster of

galaxies in this direction. The extent of this supercluster is ~ 50 Mpc along the line-of-sight and > 10 Mpc in the plane of the sky.

It is evident from the above discussion that the quasar absorption lines hold great promise for the understanding of the early universe, in particular, the nature and evolution of intergalactic medium, structure formation and evolution of galaxies, chemical evolution and large scale structure etc. The observations at present have given only qualitative information due to the large uncertainties and scatter in the data. However, improved high resolution/signal to noise ratio data are constantly being acquired and should provide more definitive information in the near future.

### References

- Acharya M., Khare P., 1993, JAA, 14,97.  
 Bahcall J., Spitzer L., 1969, ApJ, 156, L63.  
 Bajtlik S., Duncan R.C., Ostriker J.P., 1988, ApJ, 327,570.  
 Barthel P.D., 1991 in proc. of the ESO Mini-Workshop on Quasar absorption lines, p. 79.  
 Bergeron J., 1988, in QSO absorption lines: Probing the Universe, eds J.C. Blades, D.A. Trunshak & C.A. Norman, Cambridge University Press, p. 275.  
 Bergeron J., Boisse P., 1991, A&A, 243,344.  
 Bergeron J., Christiani S., Shaver P.A., 1992, A&A, 257,417.  
 Blades J.C., 1988, in QSO absorption lines: Probing the Universe, eds J.C. Blades, D.A. Trunshak, & C.A. Norman, Cambridge University Press, p. 147.  
 Bond R., Sazlay A., Silk J., 1988, ApJ, 324,627.  
 Burbidge E.M., Lynds C.R., Burbidge G.R., 1966, ApJ, 144,447.  
 Caulet A., 1989, ApJ, 340,90.  
 Foltz C.B., Weyman R.J., Roser H.J., Chaffee F.H., 1984, ApJ, 281,L1.  
 Ikeuchi S., Ostriker J.P., 1986, ApJ, 301,552.  
 Khare P., Rana N.C., 1993, JAA, 14,83.  
 Kulkarni V.P., Fall S.M., 1993, ApJ, 413,L63.  
 Lanzetta K.M., Turnshak D.A., Wolfe A.M., 1987, ApJ, 322,739.  
 Lanzetta K.M., Wolfe A.M., Turnshak D.A., Lu, L., McMahon G., Hazard C., 1991, ApJS, 77,1.  
 Lu L., Wolfe A.M., Turnshak D.A., 1991, ApJ, 367,19.  
 Peterson P. 1978, in IAU Symp: The Large Scale Structure of the Universe, eds M.S. Longair & J. Einasto, D. Reidel, Dordrecht, p. 309.  
 Pettini M., Smith L.J., Hunstead R.W., King D.L., 1994, ApJ, 426,79.  
 Rees M.J., 1986, MNRAS, 218,25p.  
 Sargent W.L.W., Boksenberg, A., Steidel C.C., 1988b, ApJS, 68,539.  
 Sargent W.L.W., Steidel C.C., Boksenberg A., 1989, ApJS, 69,703.  
 Sargent W.L.W., Steidel C.C., Boksenberg A., 1988a, ApJ, 334,22.  
 Sargent W.L.W., Young, P.J., Boksenberg A., Tytler D., 1980, ApJS, 42,41.  
 Savaglio S., D'Odorico S., Moller P. 1994, A&A, 281,331.  
 Shaver P.A., Robertson J.G., 1983, in proc. 24th Liege Symposium, Quasar and gravitational Lensing, p. 598.  
 Smette A., Surdej J., Shaver P.A., Foltz C., Chaffee F., Weyman R., Magain P., 1992, ApJ, 389,39.  
 Srikanth R., Khare P., 1993, ApJ, 413,486.

- Srianand R., Khare P., 1994, ApJ, 428,82.  
Steidel C.C., 1990, ApJS, 74,47.  
Steidel C.C., 1993, in Galaxy Evolution: The Milky Way Perspective, ed. S.R. Majewski, ASP conference series, Vol. 49, p. 227.  
Steidel C.C., Sargent W.L.W., 1992, ApJS, 80,1.  
Steidel C.C., Sargent W.L.W., Boksenberg A., 1988, ApJ, 333, L5.  
Stockton A.N., Lynds C.R., 1966, ApJ, 144,451.  
Traverse D., Giallongo E., Camurani L., 1992, ApJ, 398,491.  
Turnshek D., 1988, in QSO Absorption Lines: Probing the Universe, eds J.C. Blades D.A. Trunshak & C.A. Norman, Cambridge University Press, p. 17  
Wampler J.E., 1991, ApJ, 368,40.  
Webb B. 1987, in IAU Symp. 124, Observational Cosmology, eds A. Hewitt, G. Burbidge & L. Fang, D. Reidel, Dordrecht, p. 803.  
Yanny B., York, D.G., 1992, ApJ, 391,569.  
York D.G., Dopita M., Green R., Bechtold J., 1986 ApJ, 311,610.  
Young P., Sargent W.L.W., Boksenberg A., 1982, ApJS, 48,455.